Inorganic Chemistry

Article

pubs.acs.org/IC

DFT-Based Comparative Study about the Influence of Fluorine and Hydroxyl Anions on Opto-Electric Properties of Borate Crystals: Choice for Better Anion

Beenish Bashir,[†,‡] Bingbing Zhang,[†,‡] Ming-Hsien Lee,[†,§] Shilie Pan,*[,†] and Zhihua Yang*[,†]

[†]Key Laboratory of Functional Materials and Devices for Special Environments, Xinjiang Technical Institute of Physics and Chemistry, Chinese Academy of Sciences; Xinjiang Key Laboratory of Electronic Information Materials and Devices, 40-1 South Beijing Road, Urumqi 830011, China

[‡]University of Chinese Academy of Sciences, Beijing 100049, China

[§]Department of Physics, Tamkang University, New Taipei City 25137, Taiwan

Supporting Information

ABSTRACT: Replacing hydroxyl anions OH^- by fluorine anions F^- in borates can cause the blue shift of the UV cutoff edge and also exhibits apparent differences in nonlinear optical (NLO) properties. To clarify the intrinsic difference between OH^- anions and F^- anions, several typical borates with different types of cations (p-cations with lone-pair electrons, trivalent rare-earth, and alkaline earth metals) have been studied. The theoretical studies reveal that the blue shift in the band gap of borates with fluorine as compared to those with hydroxyl can be assumed to be the result of weaker interaction of the cation−fluoride (La/Bi/B−F) bonds compared to that of the cation-oxygen and hydroxyl bonds. NLO properties are found to have the order of BiB_2O_4F > $BiB_2O_4(OH)$> LaB_2O_4F ≈ $LaB_2O_4(OH)$. The large difference can be attributed mainly to the stereochemical activity of the lone pair (SCALP) effect of the Bi cations and the special BO_3F with strong anisotropy as compared to the BO_4 group. The energy spanning of F-2p orbitals is more extended in BiB_2O_4F as compared to LaB_2O_4F, $Sr_3B_6O_{11}F_2$, and $Ba_3B_6O_{11}F_2$ due to the bonding of Bi/B−F, which indicates F-2p orbitals have more chance to overlap with surrounding atoms and enhance the polarizability in all systems. Moreover, the degree of SCALP of the Bi cations is apparently activated by the introduction of the F^- anions, which causes an obvious enhancement in NLO properties in bismuth borates with F^-. These investigations will help us to classify the solid-state chemistry of F^- and OH^- anions in borate systems with different types of metal cations.

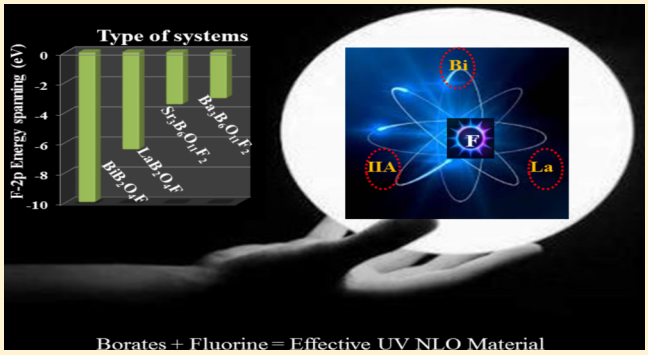

1. INTRODUCTION

For the last few decades, the noncentrosymmetric [NCS] crystals are attracting an ever increasing interest, especially for potential applications in optoelectronics.[1] The NCS borates with large second harmonic generation (SHG) effects are very promising for nonlinear optical (NLO) applications in optical parametric oscillators and large-frequency conversion efficiency lasers.[2] Especially, borates are attractive because of their IR-UV wide-range transparency and high optical quality, accompanied by their relatively high chemical and mechanical stability.[3] However, many well-known NLO systems like β-BaB_2O_4 (BBO),[4] LiB_3O_5 (LBO),[5] and $KBe_2BO_3F_2$ (KBBF)[6] have been discovered during the past few decades and used in advanced optoelectronic devices. However, it is still a big challenge to synthesize highly effective materials with prominent NLO effects.[7]

The distortion caused by the stereochemically active lone pair of p-cations (Pb^{2+}, Bi^{3+}) is one of the noticeable factors, which is responsible for the enhancement of the SHG response in $Cd_4BiO(BO_3)_3$,[8] $Pb_4O(BO_3)_2$,[9] $BiTeBO_9$,[10] $Pb_2(BO_3)(NO_3)$,[11] and $Bi_2O_2CO_3$.[12] Recently, α-BiB_3O_6 (BIBO)[13] has attracted attention for its large effective SHG coefficient (d_{eff} = 3.2 pm/V), which is due to heavily distorted Bi polyhedra $(BiO_4)^{5-}$; however, its low symmetry (space group Cm) largely restricts its applications in optoelectronic devices.[14] So it is necessary to explore other Bi^{3+}-containing compounds for desirable applications. Furthermore, the introduction of VII-A group elements increases the distortion of the metal cations (Pb^{2+}, Bi^{3+}) as in $Pb_2B_5O_9I$,[15] $Pb_2TiOF(SeO_3)_2Cl$,[16] $BiFSeO_3$,[17] $BaBi(SeO_3)_2Cl$,[18] $PbPt(IO_3)_6(H_2O)$,[19] and $Bi_7F_{11}O_7$.[20]

Thus, the compounds which have distorted metal p-cations with VII-A group elements enhance the local dipole moments and increase the overall electric susceptibility.[18,21] Moreover, VII-A group anions may also serve as structure-directing agents to construct NCS frameworks by aligning different asymmetric

Received: January 15, 2017
Published: April 27, 2017

DOI: 10.1021/acs.inorgchem.7b00120
Inorg. Chem. 2017, 56, 5636−5645

units in the same direction to form a macroscopic polar system.[22] Alongside the (Pb^{2+}, Bi^{3+}) cations with the SCALP effect, the introduction of alkaline earth metals and trivalent rare-earth metals are also considered as promising UV/deep−UV optical systems because they have no d−d and f−f electronic transitions, like $Na_3La_9O_3(BO_3)_8$,[23] $La_2CaB_{10}O_{19}$,[24] $Na_3La_2(BO_3)_3$,[25] $Na_8Lu_2(CO_3)_6F_2$,[26] $Na_3Lu(CO_3)_2F_2$,[26] $Ba_2B_{10}O_{17}$,[27] $BaCaBO_3F$,[28] $Ca_5(BO_3)_3F$,[29] and $M_3B_6O_{11}F_2$ (M = Sr, Ba).[30]

The main objective of this work is not only to evaluate optical properties of bismuth borate systems but also to concentrate on the first-principles electronic structures effected by the introduction of fluorine anions and hydroxyl groups in different nature of cations borate systems like BiB_2O_4F,[31] $BiB_2O_4(OH)$,[31b] LaB_2O_4F, $LaB_2O_4(OH)$, and $M_3B_6O_{11}F_2$ (M = Sr, Ba)[30] systems. The following points will be discussed in this work:

1. How do optical features of systems originate from the electronic structure point of view in bismuth borate systems?
2. How do the F and OH units affect the band gap topology, electronic structure, and optical properties of systems? Is the influence of F and OH anions related to the nature of cations in borate systems?

Generally, the introduction of the F atoms into metal borates, by the replacement of the O atoms or the OH group, leads to variations in structure, where the F ions form bridging and terminal bonds involving metal polyhedra.[32] The introduction of F also has a positive effect on designing and synthesizing new borates as frequency-doubling (FD) materials like $Ba_4B_{11}O_{20}F$,[33] $Na_3Ba_2(B_3O_6)_2F$,[34] $NaSr_3Be_3B_3O_9F_4$,[35] $Li_3Ca_9(BO_3)_7{\cdot}2[LiF]$,[36] and $LiBa_{12}(BO_3)_7F_4$.[37] It has been previously reported that the OH group causes unfavorable effects as compared to halides on optical nonlinearity.[38] Thus, both anions (F and OH) in an identical borate framework behave differently and affect the properties of borate systems. In this regard, first-principles-based scientific research is very supportive to explore the knot between the electronic structure and optical properties of systems.[39] In this research work, theoretical tools including electronic structure analysis, SHG-density,[40] and band-resolved method[41] are adopted.

2. THEORETICAL METHODOLOGY

Based on density functional theory (DFT), the CASTEP module,[42] a plane-wave pseudo-potential was used to investigate the optoelectronic properties of investigated systems. The generalized gradient approximation (GGA),[43] with the exchange correlation functional Perdew−Burke−Ernzerhof (PBE),[44] and norm conserving pseudopotential (NCP),[44b] has been adopted for BiB_2O_4F, $BiB_2O_4(OH)$, LaB_2O_4F, and $LaB_2O_4(OH)$ systems. The energy cutoff, E_{cutoff} = 850 eV, and Monkhorst−Pack k-point meshes,[45] spanning with less than 0.04 $Å^{-3}$ separation, were applied. Geometries were optimized using convergence thresholds for the total energy, maximum force, and displacement as 5.0×10^{-6} eV/atom, 0.01 eV/Å, and 5×10^{-4} Å, respectively. On the basis of optimized geometry, the electronic and optical properties were investigated. The convergent criteria with other parameters have been kept as default settings for the CASTEP code. The convergence results proved that the preceding computational setting was reasonable for the investigation of opto-electric properties of the studied systems. Usually, the theoretically calculated band gap is underestimated because of the existence of discontinuity within generalized gradient approximation (GGA) related with excitation energies in DFT method.[44c,46] Therefore, the scissors operator,[46a,47] for correction of gap by transmitting all the conduction bands far away from the valence bands (VBs), was applied during the calculation of optical properties.

The modified form of static second order coefficients ${\chi_{\alpha\beta\gamma}}^{(2)}$ is described as[48]

$$ {\chi_{\alpha\beta\gamma}}^{(2)} = {\chi_{\alpha\beta\gamma}}^{(2)}(\mathrm{VE}) + {\chi_{\alpha\beta\gamma}}^{(2)}(\mathrm{VH}) \tag{1} $$

whereas virtual electron (VE) and virtual hole (VH) contributions are as follows:

$$ {\chi_{\alpha\beta\gamma}}^{(2)}(\mathrm{VE}) = \frac{e^3}{2\hbar^2 m^3} \sum_{vcc'} \int \frac{d^3k}{4\pi^3} P(\alpha\beta\gamma)\mathrm{Im}[P^{\alpha}_{vc}P^{\beta}_{cc'}P^{\gamma}_{c'v}] \left(\frac{1}{\omega^3_{cv}\omega^2_{vc'}} + \frac{2}{\omega^4_{vc}\omega_{c'v}}\right) \tag{2} $$

$$ {\chi_{\alpha\beta\gamma}}^{(2)}(\mathrm{VH}) = \frac{e^3}{2\hbar^2 m^3} \sum_{vv'c} \int \frac{d^3k}{4\pi^3} P(\alpha\beta\gamma)\mathrm{Im}[P^{\alpha}_{vv'}P^{\beta}_{v'c}P^{\gamma}_{cv}] \left(\frac{1}{\omega^3_{cv}\omega^2_{v'c}} + \frac{2}{\omega^4_{vc}\omega_{cv'}}\right) \tag{3} $$

where α, β, and γ are Cartesian elements, v and v' are valence bands, c and c' symbolize conductions bands, $P(\alpha\beta\gamma)$ indicates full permutation, and P_{ij}^{α} describes the momentum matrix components.

To sort out the participation of every electronic orbital (i.e., occupied and unoccupied bands) toward the total SHG response, the band-resolved method has been executed. The integral SHG with respect to energy region can be achieved to acquire the knowledge about dominant participation of various orbitals to overall $\chi^{(2)}$. To further analyze the origins of SHG response in studied systems, the SHG density method has been employed. Through the SHG density method, the contribution of ions or groups in the system that take their part to improve the NLO properties can be explored. The proceeding theoretical methodology has been proved to be successful in various NLO systems to evaluate the SHG effect.[49]

3. RESULTS AND DISCUSSION

3.1. Crystal Structure and Stereochemical Activity of Bismuth Cations. The crystal data details about BiB_2O_4F,[31] $BiB_2O_4(OH)$,[31b] LaB_2O_4F, $LaB_2O_4(OH)$, $Sr_3B_6O_{11}F_2$,[30] and $Ba_3B_6O_{11}F_2$[30] are, respectively, given in Table S1 in the Supporting Information (SI). BiB_2O_4F and $BiB_2O_4(OH)$ crystallize in the trigonal space group $P3_2$ and $P3_1$, respectively, with tetrahedral borate groups and distorted BiO_5 polyhedra. In BiB_2O_4F, the borate framework is composed of two BO_4 and one BO_3F subunits, combined together through corner sharing to build the B_3O_8F ring as a fundamental building block (FBB) and further interconnected by the Bi cations to form 3-D network crystal structure. Thus, the Bi cations reside in the cavities of borate framework. During the studies two new virtual structures (LaB_2O_4F with $P3_2$ and $LaB_2O_4(OH)$ with $P3_1$) obtained by substituting Bi with La in BiB_2O_4F and $BiB_2O_4(OH)$, which are dynamically stable as shown in Figure S1 in the SI with respect to phonon dispersion, are investigated as references. In LaB_2O_4F, F is connected with the La cation

DOI: 10.1021/acs.inorgchem.7b00120
Inorg. Chem. 2017, 56, 5636−5645

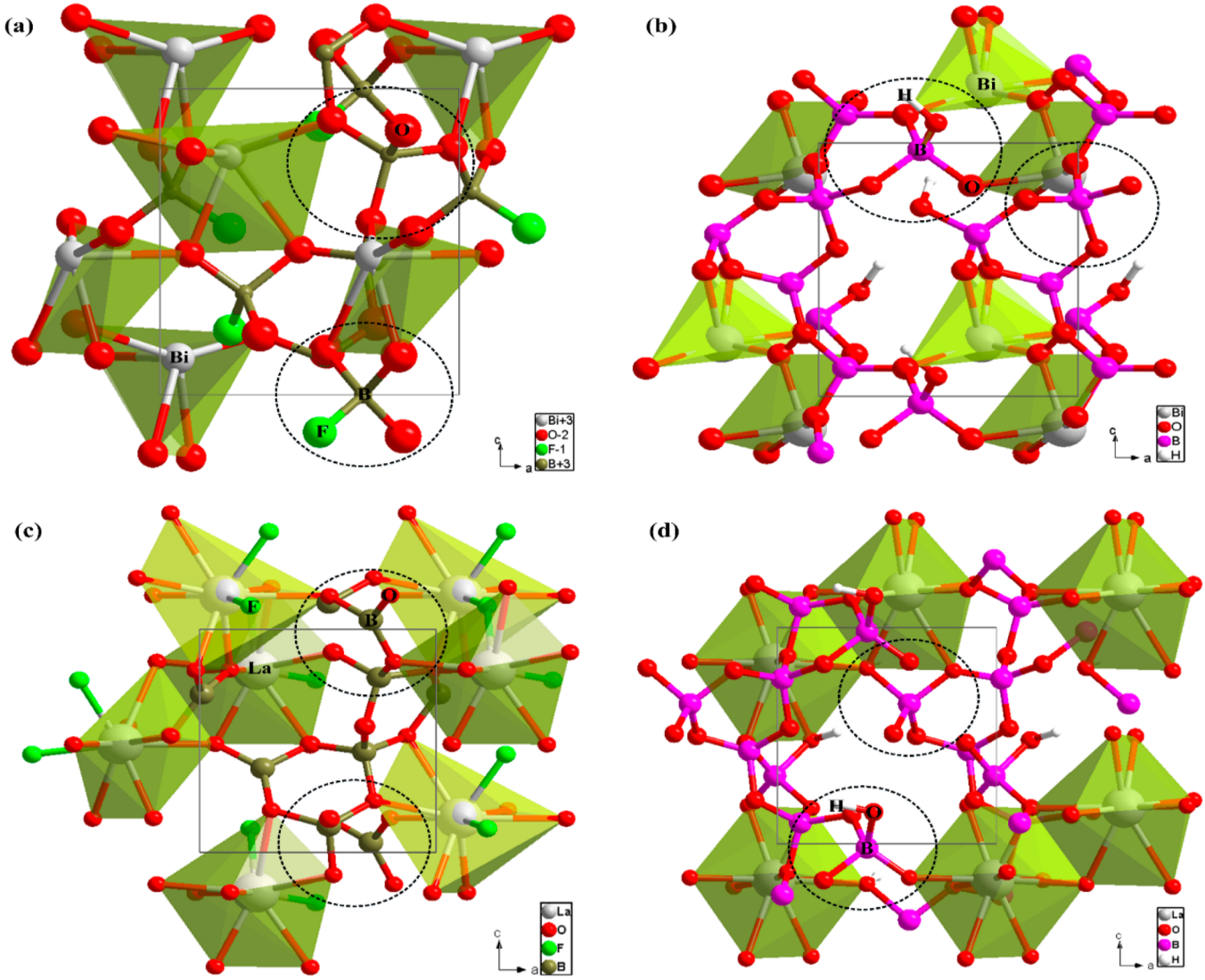

Figure 1. Structure description of (a) BiB_2O_4F, (b) $BiB_2O_4(OH)$, (c) LaB_2O_4F, (d) $LaB_2O_4(OH)$. Bi/La, F, and OH are located in the voids of the borate framework.

only instead of being part of the B−O framework, as in case of BiB_2O_4F; thus, two BO_4 and one BO_3 are combined through corner sharing to build a B_3O_8 ring as FBB. $BiB_2O_4(OH)$/$LaB_2O_4(OH)$ have quite similar structure features like BiB_2O_4F/LaB_2O_4F, except the replacement of the F anions with the OH anions as shown in Figure 1. For the isostructural borate fluorides $M_3B_6O_{11}F_2$ (M= Sr, Ba) with the space group $P2_1$, two BO_3 and four BO_4 form the B_6O_{14} FBB, and the Sr/Ba cations and the F anions are placed in the voids of borate framework to form 3D network crystal structures.

The F and OH anions induce the crystal structure properties and NLO susceptibility in such a manner that BiB_2O_4F has 2 times larger SHG response (~12 × KDP) than $BiB_2O_4(OH)$ (~6 × KDP), whereas LaB_2O_4F and $LaB_2O_4(OH)$ have the SHG response ~1 × KDP. Therefore, it is interesting to know that the F and OH anions behave quite differently in two bismuth borates. Generally, owing to higher electron affinity and smaller size of the F anions in comparison with the O atoms, the F anions cause more polarizability in the BO_3F tetrahedron as compared to the BO_4 tetrahedron.[50] Similarly, the M−F (M = metal) bond as compared to the M−O bond can largely enhance the anisotropic value for microscopic susceptibility.[49c] Thus, the bonding of F anions plays an important role in SHG factors. In addition, the SCALP effect causes distortion in the cation centered polyhedra, represented by the analyzed oxygen (O) distribution around bismuth in Figure S2 in the SI. The BiO_5 polyhedron is considerably asymmetric with Bi−O unequal bond length ranging from 2.24 to 2.54 Å in BiB_2O_4F, and 2.15−2.69 Å in $BiB_2O_4(OH)$. Comparison of the BiO polyhedron of BiB_2O_4F, with those of $BiB_2O_4(OH)$, $CaBi_2B_2O_7$,[51] and $BaBiBO_4$,[52] shows that the Bi-centered polyhedron (BiO_5) shows remarkably greater distortions in BiB_2O_4F, and it is evident from angle reduction for O−Bi−O (55°−145°) in BiB_2O_4F as compared to O−Bi−O (59°−166°) in $BiB_2O_4(OH)$, (55°−167°) in $CaBi_2B_2O_7$, and (58°−170°) in $BaBiBO_4$. For further confirmation, the magnitude of distortion (Δd) is calculated,[53] which is 4.244 for BiB_2O_4F and 2.985 for $BiB_2O_4(OH)$. Thus, it is clear that the strong distortion is beneficial to the large SHG response, such as in BiB_2O_4F (~2 × $BiB_2O_4(OH)$). While in LaB_2O_4F, F is just connected with the La cation and does not cause anisotropy in B−O framework. Thus, overall susceptibility in LaB_2O_4F and $LaB_2O_4(OH)$ is almost the same, which leads to an identical SHG response.

DOI: 10.1021/acs.inorgchem.7b00120
Inorg. Chem. 2017, 56, 5636−5645

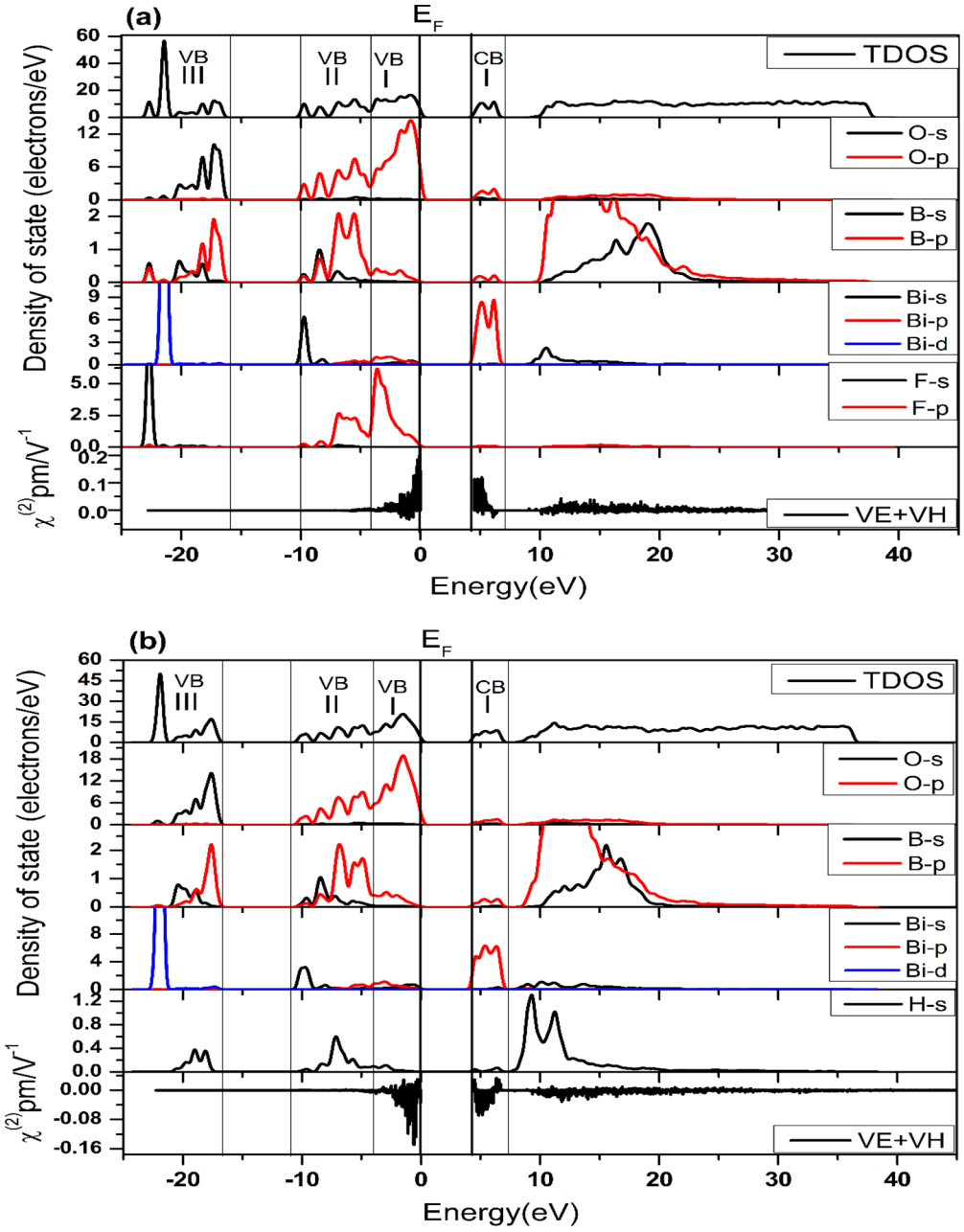

Figure 2. PDOS with band-resolved $\chi^{(2)}$ of (a) BiB_2O_4F (b) $BiB_2O_4(OH)$. Band-resolved $\chi^{(2)}$ with integral value of VE+VH indicate the prominent regions VB-I and CB-I that participate in the SHG coefficient in respective systems.

Now the remaining question is the following: Despite similar coordination environment and the arrangement of the lone pair along *c*-axis in the two bismuth borates, how is the extent of distortion in Bi−O polyhedra different? The structural parameters show that enhancement of the distortion is mainly due to presence of the F anions that cause the anisotropy in the BiO_5 polyhedra in BiB_2O_4F. The distortion caused by halogens in cation centered polyhedra like in $Pb_2B_5O_9I$,[15] $Ba_4B_{11}O_{20}F$,[33] Pb_2BO_3F,[54] HdpaNbOF$_4$ (dpa = 2,2′-dipyridylamine),[55] $Bi_2WO_{6-x}F_{2x}$,[56] $Bi_3OF_3(IO_3)_4$,[57] $NaVO_{2-x}F_{2+x}$ (x = 1/3),[58] and Na_2SbF_5[59] is also observed. The polarization effect of anions can play a significant role to enhance overall susceptibility of system.[33] Thus, according to the flexible dipole model, the second-order polarizability of system is significantly increased by the introduction of different electron-withdrawing atoms/group like F, CF_3, and CN.[60] F has an electron-withdrawing ability because of its large electronegativity, whereas OH has electron-donating capability; therefore, they affect not only the crystal structure but also the optical properties of crystals in contrasting fashion. In order to better explain the behavior of F and OH under different cations in borate systems, density-functional-theory-based theoretical calculations were performed, and we obtained in-depth knowledge regarding the structural properties for the studied NLO materials.

3.2. Comparison of Electronic Structures and Effect of Anions (F vs OH) under Different Cations. The results of band gap calculations (Table S2 in the SI) indicate that BiB_2O_4F, and $BiB_2O_4(OH)$ are indirect band gap materials with the value of 4.21 eV (experimental band gap 4.43 eV) and 4.06 eV (experimental band gap 4.28 eV), respectively. In the case of virtual systems LaB_2O_4F and $LaB_2O_4(OH)$, both have indirect

DOI: 10.1021/acs.inorgchem.7b00120
Inorg. Chem. 2017, 56, 5636−5645

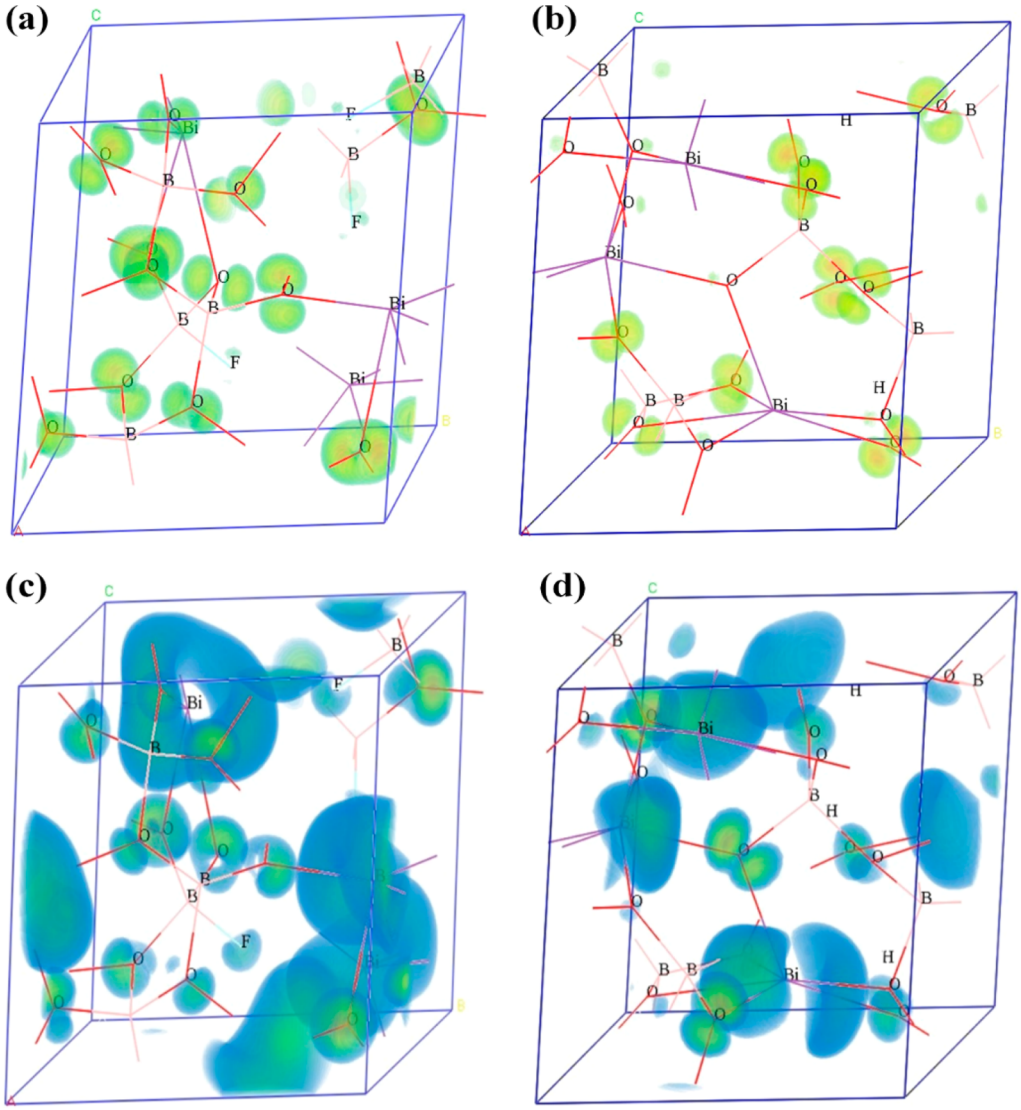

Figure 3. Atomic orbitals at VBM regions (a,b) and CBM regions (c,d) of BiB_2O_4F and $BiB_2O_4(OH)$, respectively.

band gaps of 6.66 eV (8.49 eV from the HSE06 result) and 6.11 eV (7.86 eV from the HSE06 result), respectively. Generally speaking, bismuth borate systems have narrow band gap like α-BiB_3O_6,[13] $CaBi_2B_2O_7$,[51] and $BaBiBO_4$,[52] as shown in Table S3 in the SI. It has been observed that the M−F bonds may have a wider optical transmission range as compared to the M−O bonds, and thus, the F anions will lead to blue shift of the transmission spectrum, like a larger band gap.[20] Also, replacing OH by F in BiB_2O_4F/LaB_2O_4F increases the band gap and is attributed to weak interaction or ionic bonding between Bi/B/La−F as compared to Bi/B/La−O and O−H bonds in $BiB_2O_4(OH)/LaB_2O_4(OH)$.[61]

The information gathered through the PDOS and their contribution in $\chi^{(2)}$ obtained from the band-resolved method of BiB_2O_4F and LaB_2O_4F is also plotted in comparison with those of $BiB_2O_4(OH)$ and $LaBO_4(OH)$, as shown in Figure 2 and Figure S3 in the SI. On the basis of the disparity in the band-resolved $\chi^{(2)}$, the DOS and PDOS are distributed into different energy regions. In BiB_2O_4F and $BiB_2O_4(OH)$, the VB-III (−23 to −16.5 eV) consists of Bi-5d and O-2s orbitals with little mixing of B-2s2p and F-2s/H-1s orbitals, whereas in LaB_2O_4F and $LaB_2O_4(OH)$, the region VB-III (below −16 eV) occupies O-2s and B-2s2p states. The VB-II (−10.5 to −4 eV) is composed of Bi-6s/La-5d with O-2p and B-2s2p orbitals, and F-2p orbitals exist in BiB_2O_4F. The VB-I (−4 eV to Fermi level) is dominated by O-2p, F-2p orbitals with slight mixing of Bi-6s6p/La-5d orbitals. The borates with the F or OH anions show similar structural features, but the presence of F-2p orbitals makes a difference, especially in VB-I. Conduction band (CB)-I is mainly composed of Bi-6p/La-5d orbitals with a small contribution from O-p, hybrid B-2s2p orbitals with a difference in the presence of F-2p and H-1s orbitals in respective BiB_2O_4F/LaB_2O_4F vs $BiB_2O_4(OH)/LaB_2O_4(OH)$. It should be noted that the behavior of the B atoms is found to be quite diverse in different B−O units. BO_3F and $BO_3(OH)$ peaks offer a greater contribution to the SHG response as compared to BO_4 in BiB_2O_4F and $BiB_2O_4(OH)$. Additionally, the BO_3 peak in LaB_2O_4F near the bottom of CB offers a greater contribution to the SHG response in comparison with PDOS of B in $BO_3(OH)$ and BO_4, as shown in Figure S4 in the SI.

In fact, covalent interaction between Bi−O/La-O shows a dominant role to energy band gap, but the influence of F cannot be ignored. Therefore, the weak interaction of F with Bi/La atoms decreases the energy of VB, which causes a blue

DOI: 10.1021/acs.inorgchem.7b00120
Inorg. Chem. 2017, 56, 5636−5645

shift of the band gap in BiB_2O_4F/LaB_2O_4F as compared to $BiB_2O_4(OH)/LaB_2O_4(OH)$. Theoretically, it is found that the F atoms need more electronic excitation energy as compared to the O atoms due to their larger electronegativity, and comparatively smaller size, and hence, they are capable of extending the transparency window in the UV range. The electronic structure and PDOS analysis show that optical absorption around the Fermi level is mainly occurring from occupied O-2p, F-2p (major) with Bi-sp/La-5d to unoccupied Bi-6p/La-5d (major), B-sp, and O-2p in BiB_2O_4F/LaB_2O_4F and from occupied O-2p (major) with Bi-sp/La-5d to unoccupied Bi-6p/La-5d (major), B-sp, O-2p, and H-1s in $BiB_2O_4(OH)/LaB_2O_4(OH)$.

The bond order is obtained to get more insight into nature of chemical bonds due to its large influence on NLO susceptibility.[62] In BiB_2O_4F, the calculated bond orders for Bi−O, Bi−F, B−O, and B−F are 0.08−0.15 e, 0.03−0.04 e, 0.60−0.67 e, and 0.45 e, respectively. The bond length of B−F (1.39 Å) is shorter than that of Bi−F (2.85−2.98 Å). Therefore, the interaction between B−F is stronger than that of Bi−F. However, compared with B/Bi−O bonds, the B/Bi−F bonds have relatively weak interactions. In $BiB_2O_4(OH)$, the calculated bond orders for Bi−O, B−O, and O−H are 0.04−0.15 e, 0.60−0.67 e, and 0.65 e, respectively, which have covalent character as shown in Table S4 in the SI. The band structure from Figure S5 in the SI shows that especially CB-I is quite parallel in BiB_2O_4F, which is due to weak interaction between orbitals of Bi−F and B−F bonds, whereas comparatively dispersive CB-I in $BiB_2O_4(OH)$ is due to comparatively strong covalent interaction between orbitals of Bi−O, B−O, and O−H bonds. Similar band structure topology has been observed in LaB_2O_4F and $LaB_2O_4(OH)$. Figure S5 in the SI shows that the weak interaction between La−F in LaB_2O_4F makes the CB-I region quite parallel, whereas the strong covalent interaction between La−O, B−O, and O−H in $LaB_2O_4(OH)$ makes the CB-I comparatively dispersive. Hoffmann[63] showed that band dispersions are determined by the interunit cell overlapping of atomic orbitals like bandwidth. The total electronic charge density map about all atoms in the system, shown in Figure S6 in the SI, suggests that the substitution of OH with F makes the difference in bonding nature that influences the band structure features.

The mixing between O-2p and hybrid Bi-6s6p orbitals shows the SCALP effect of the Bi cations in both bismuth borate systems, that is, according to the Payne revised model.[64] The presence of F-2p orbitals in this energy region further enhances this effect, as shown in Figure 2a. The degree of SCALP (R)[53,65] is calculated to be 0.1631 for BiB_2O_4F and 0.12742 for $BiB_2O_4(OH)$. The large R value for BiB_2O_4F is due to presence of the F anions that increase the intrinsic SCALP effect of the Bi polyhedra. In contrast, the OH anions with intrinsic electron-donating ability supersaturate the polarizability of neighboring atoms under incident light, which depress the overall polarizability and NLO response of the system.[30] Hence, the OH anions cannot withdraw lone pairs of the Bi cations to increase the distortion in $BiB_2O_4(OH)$. Ultimately, the spatial susceptibility caused by the F anions in BiB_2O_4F is depressed by the OH anions in $BiB_2O_4(OH)$, which leads to a small SHG response. The electron distribution between Bi−O and borate framework is examined, which shows that the Bi−O bond in BiB_2O_4F has more delocalization character than that in $BiB_2O_4(OH)$, as shown in Figure 3. Interestingly, the O atoms connected with $BO_3F/BO_3(OH)$ are more delocalized than those connected with BO_4. Recent work has proved that the BO_3F groups are good NLO functional units as compared to BO_4 because of the enhancement of polarizability.[50] Thus, the combination of BO_3F with Bi having a greater SCALP effect holds higher polarizability and leads to a larger SHG response. However, the difference in the delocalization character between LaB_2O_4F and $LaB_2O_4(OH)$ is not really obvious, as shown in Figure S7 in the SI, and similar results can also be found in alkaline-metal borate fluorides such as in $M_3B_6O_{11}F_2$ (M = Sr, Ba). So it is necessary to clarify the effect of anions under different cations.

Figure 4 shows that in BiB_2O_4F, LaB_2O_4F, and $M_3B_6O_{11}F_2$ (M = Sr, Ba) the energy spanning of the F anion is −10 to 0 eV, −6.5 to 0 eV, and −3.3 to 0 eV, respectively. In BiB_2O_4F, as F is connected with B and also with Bi, so the energy spanning is more extended. Resultant F anions cause anisotropy in BO_3F and facilitate the SCALP effect of Bi-centered polyhedra. Thus, the bonding of the F anions causes a greater polarization effect in the system, which plays an important role in the enhancement of the NLO response. In LaB_2O_4F and $M_3B_6O_{11}F_2$ (M = Sr, Ba), the energy spanning is comparatively less extended due to the bonding of F with the La/Sr/Ba cations, so F just has the chance to cause the polarizability in La/Sr/Ba-centered polyhedra. These results are consistent with the above molecular viewpoint discussion. It can be concluded that the F anions act as active participant for the blue shift of band gap in studied systems than the OH anions and especially good choice in bismuth borates for enhancement of SCALP effect, which leads to large SHG effect.

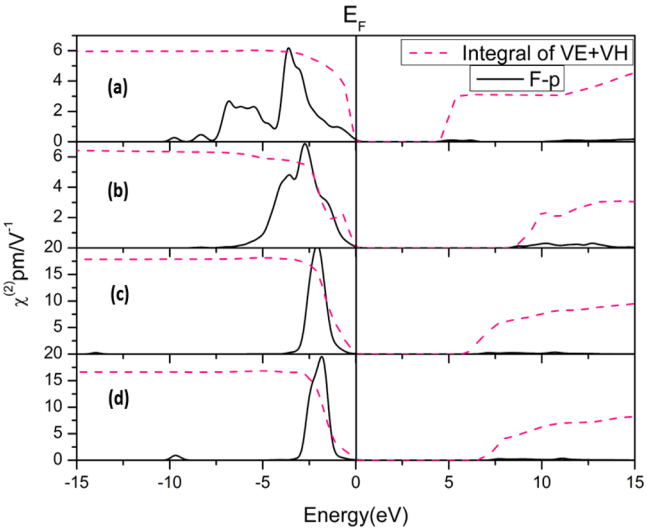

Figure 4. Comparison of energy spanning of F-p orbitals through PDOS and integral of VE+VH (Pink line) in (a) BiB_2O_4F, (b) LaB_2O_4F, (c) $Sr_3B_6O_{11}F_2$, and (d) $Ba_3B_6O_{11}F_2$ systems.

3.3. SHG Density Analysis. The theoretically calculated SHG coefficients for BiB_2O_4F, $BiB_2O_4(OH)$, LaB_2O_4F, and $LaB_2O_4(OH)$ are enlisted with their experimental counterparts in Table S5 in the SI. Theoretical values being pretty close to the experimental values are an evidence of the application accuracy of first-principles methods. Also, the SHG density method is used to sort out the contributions of anions to the second-order susceptibility, which also determines the cumulative contributions from VE and VH processes. Also, irrespective to the role of VE process for the determination

DOI: 10.1021/acs.inorgchem.7b00120
Inorg. Chem. 2017, 56, 5636−5645

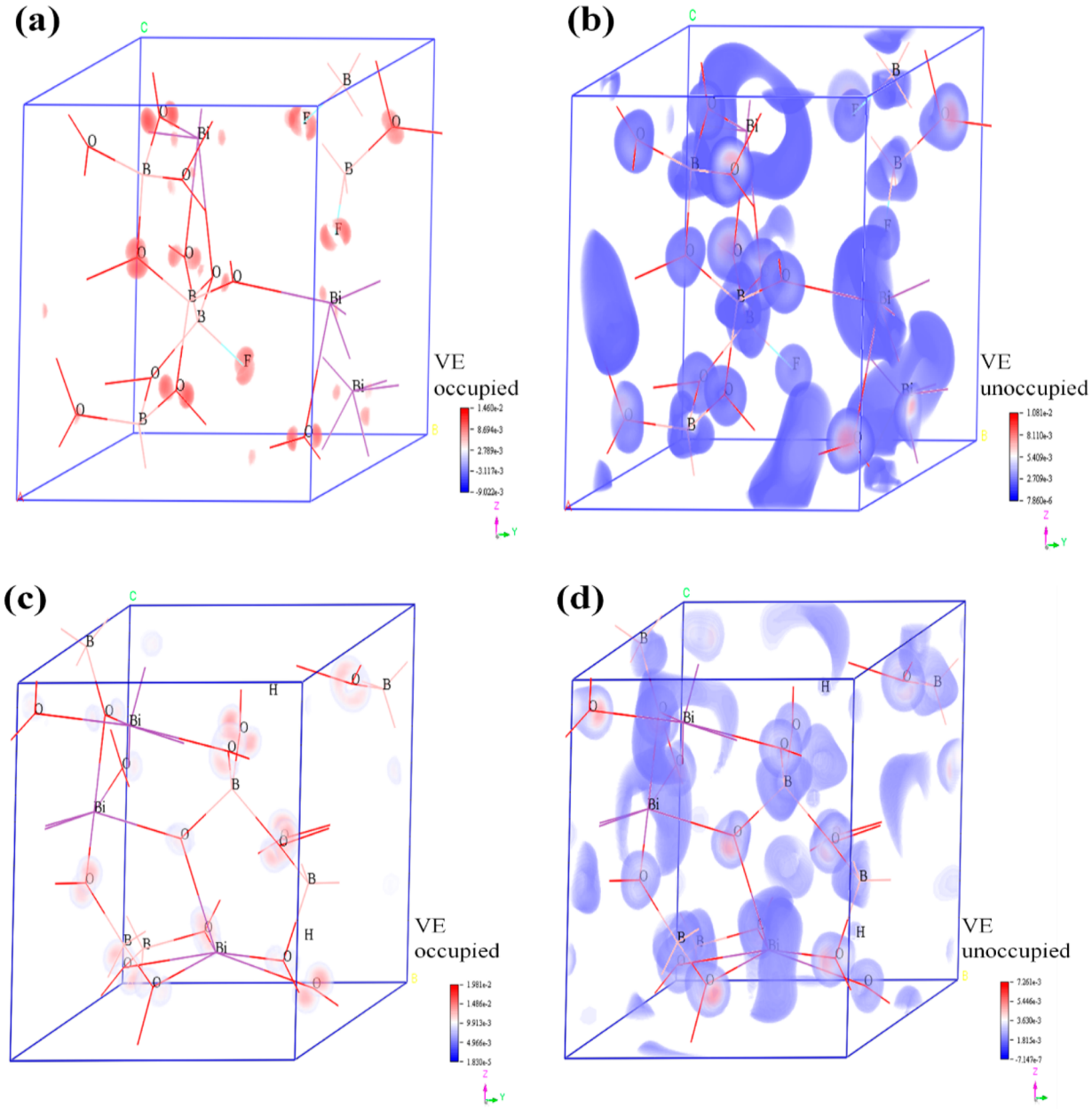

Figure 5. SHG densities of VE process for BiB_2O_4F (a,b) and $BiB_2O_4(OH)$ (c,d).

of the occupied states, the current study is focused on its contribution in defining the SHG effect.

To investigate the origins of the strong SHG effect for both studied systems, we performed further analysis of the SHG densities. From Figure 5, it can be clearly observed that the 2p orbitals of all the O atoms give the prominent contribution to the SHG in the VB. The SHG density around the F anions also shows its non-negligible contribution in BiB_2O_4F. However, in $BiB_2O_4(OH)$, the O atoms, which are linked with H atoms, give more dominant contribution. In the CB, the SHG effect is mainly contributed by unoccupied Bi-6p and O-2p orbitals, mixing with some F-2p and B-2p orbitals in BiB_2O_4F and H-1s orbitals in $BiB_2O_4(OH)$. Figure S8 in the SI shows the similar results of SHG densities of LaB_2O_4F and $LaB_2O_4(OH)$. The SHG density around the Bi cation in BiB_2O_4F shows more prominent contribution as compared to Bi in $BiB_2O_4(OH)$. On the basis of electronic structure and SHG density analyses, it is concluded that the Bi−O groups have a dominant role in SHG response in studied materials like α-BiB_3O_6,[13] $CaBiB_2O_7$,[51] and $BaBiB_2O_4$.[52] The presence of the F anions acts as motivating source to enhance polarizability and SCALP effect which influence the SHG response more prominently instead of the OH anions in BiB_2O_4F. The contribution of the F anions in LaB_2O_4F for widening the transparency window in the UV range is larger than that in $LaB_2O_4(OH)$, even though the influence of F and OH toward SHG response in both crystals is the same.

On the basis of theoretical studies based on electronic structure, PDOS, and SHG density analyses, it is concluded that the Bi−O groups have a dominant role in the SHG response in bismuth borate systems. However, the incorporation of the opposite nature of anions (F, OH) is the main source of diversity in SHG response of BiB_2O_4F and $BiB_2O_4(OH)$. Finally, it has been concluded that the F anions in comparison to the OH anions are the better choice for the synthesis of high-performance effective NLO bismuth borates.

DOI: 10.1021/acs.inorgchem.7b00120
Inorg. Chem. 2017, 56, 5636−5645

4. CONCLUSIONS

In conclusion, the role of anions (F, OH) under different nature of cations including BiB_2O_4F, $BiB_2O_4(OH)$, LaB_2O_4F, $LaB_2O_4(OH)$, and $M_3B_6O_{11}F_2$ (Sr, Ba) systems are studied through DFT calculation. The band gap is found to be larger in BiB_2O_4F/LaB_2O_4F than that in $BiB_2O_4(OH)/LaB_2O_4(OH)$ and can be assumed to be the result of weak interaction of the Bi/B/La−F bonds in comparison to the Bi/B/La−O and hydroxyl bonds. The SHG responses of different crystals under study are in the order of BiB_2O_4F > $BiB_2O_4(OH)$> $LaB_2O_4F \approx LaB_2O_4(OH)$. The greater SHG response of BiB_2O_4F as compared to $BiB_2O_4(OH)$ is due to the SCALP effect of Bi and the greater anisotropy of BO_3F than that of the BO_4 group. Thus, the presence of the F anions triggers the SCALP effect of Bi, which is beneficial to the optical anisotropy combined with the B−F bonds in BO_3F. Irrespective of similar contribution of the F and OH anions in LaB_2O_4F and $LaB_2O_4(OH)$ crystals for SHG response, the F anions induce a larger transparency window in the UV range as compared to OH anions in respective crystals. The energy spanning of F-2p orbitals is more expanded in BiB_2O_4F as compared to LaB_2O_4F, $Sr_3B_6O_{11}F_2$, and $Ba_3B_6O_{11}F_2$. This spanning of energy is due to the bonding of Bi/B−F, which indicates F-2p orbitals have greater chance to overlap with surrounding atoms and enhance the polarizability that plays an important role in SHG factors in BiB_2O_4F. The main objective of the present contribution is to work out the principle features of the F anions, as it can offer an encouraging effect on the structural properties of the borate systems. Thus, the present contribution may offer novel, broader, and exploratory insight into the manufacture of borates that contain the F anions because of the advantages they offer, especially in the UV and DUV region. Also, upcoming studies may seek an insight for better exploration of new frequency-doubling systems to meet future industry demands.

■ ASSOCIATED CONTENT

Supporting Information

The Supporting Information is available free of charge on the ACS Publications website at DOI: 10.1021/acs.inorgchem.7b00120.

Crystal detail; theoretical band gap values; SHG coefficient and selected bond distances of BiB_2O_4F and $BiB_2O_4(OH)$; theoretical band gap values of α-BiB_3O_6, $CaBiB_2O_7$, and $BaBiB_2O_4$; phonon dispersion of LaB_2O_4F and $LaB_2O_4(OH)$; the Bi−O polyhedra in BiB_2O_4F, $BiB_2O_4(OH)$, $CaBi_2B_2O_7$, and $BaBiBO_4$; electronic structures of LaB_2O_4F and $LaB_2O_4(OH)$; PDOS of B−O framework; band structures; total charge density map and of BiB_2O_4F and $BiB_2O_4(OH)$; atomic orbitals at CBM of LaB_2O_4F and $LaB_2O_4(OH)$; and SHG densities in VE for LaB_2O_4F and $LaB_2O_4(OH)$ (PDF)

■ AUTHOR INFORMATION

Corresponding Authors

*E-mail for Z.Y.: zhyang@ms.xjb.ac.cn. Tel.: (+86)-991-3810816. Fax: (+86)-991-3838957.

*E-mail for S.P.: slpan@ms.xjb.ac.cn.

ORCID

Shilie Pan: 0000-0003-4521-4507

Zhihua Yang: 0000-0001-9214-3612

Notes

The authors declare no competing financial interest.

■ ACKNOWLEDGMENTS

This work is supported by National Basic Research Program of China (Grant No. 2014CB648400), the National Key Research Project (Grant Nos. 2016YFB1102302, 2016YFB0402104), the National Natural Science Foundation of China (Grant No. 11474353,51425206), the Xinjiang Program of Cultivation of Young Innovative Technical Talents (Grant No. qn2015jq013). Xinjiang Program of Introducing High-Level Talents. Authors are also encouraged by CAS−TWAS President Fellowship for academic support.

■ REFERENCES

(1) Wolynski, A.; Herrmann, T.; Mucha, P.; Haloui, H.; L'huillier, J. Laser Ablation of CFRP Using Picosecond Laser Pulses at Different Wavelengths from UV to IR. *Phys. Procedia* **2011**, *12*, 292−301.

(2) (a) Zhang, W.; Xiong, R.-G. Ferroelectric Metal−Organic Frameworks. *Chem. Rev.* **2012**, *112*, 1163−1195. (b) Becker, P. Borate materials in nonlinear optics. *Adv. Mater.* **1998**, *10*, 979−992.

(3) Ok, K. M.; Chi, E. O.; Halasyamani, P. S. Bulk characterization methods for non-centrosymmetric materials: second-harmonic generation, piezoelectricity, pyroelectricity, and ferroelectricity. *Chem. Soc. Rev.* **2006**, *35*, 710−717.

(4) (a) Chen, C. T.; Wu, B.; Jiang, A.; You, G. A new-type ultraviolet SHG crystal: β-BaB_2O_4. *Sci. Sin. B* **1985**, *28*, 235−243. (b) French, R. H.; Ling, J. W.; Ohuchi, F. S.; Chen, C. T. Electronic structure of β-BaB_2O_4 and LiB_3O_5 nonlinear optical crystals. *Phys. Rev. B: Condens. Matter Mater. Phys.* **1991**, *44*, 8496−8502.

(5) Xie, F.; Wu, B.; You, G.; Chen, C. T. Characterization of LiB_3O_5 crystal for second-harmonic generation. *Opt. Lett.* **1991**, *16*, 1237−1239.

(6) Lin, Z. S.; Wang, Z. Z.; Chen, C. T.; Chen, K. S.; Lee, M.-H. Mechanism for linear and nonlinear optical effects in $KBe_2BO_3F_2$ (KBBF) crystal. *Chem. Phys. Lett.* **2003**, *367*, 523−527.

(7) Chen, C. T.; Lin, Z.; Wang, Z. The development of new borate-based UV nonlinear optical crystals. *Appl. Phys. B: Lasers Opt.* **2005**, *80*, 1−25.

(8) Zhang, W.-L.; Cheng, W.-D.; Zhang, H.; Geng, L.; Lin, C.-S.; He, Z.-Z. A strong second-harmonic generation material $Cd_4BiO(BO_3)_3$ originating from 3-chromophore asymmetric structures. *J. Am. Chem. Soc.* **2010**, *132*, 1508−1509.

(9) Yu, H. W.; Pan, S. L.; Wu, H. P.; Zhao, W. W.; Zhang, F. F.; Li, H. Y.; Yang, Z. H. A new congruent-melting oxyborate, $Pb_4O(BO_3)_2$ with optimally aligned BO_3 triangles adopting layered-type arrangement. *J. Mater. Chem.* **2012**, *22*, 2105−2110.

(10) Xia, M.; Jiang, X.; Lin, Z.; Li, R. All-Three-in-One": A New Bismuth-Tellurium-Borate Bi_3TeBO_9 Exhibiting Strong Second Harmonic Generation Response. *J. Am. Chem. Soc.* **2016**, *138*, 14190−14193.

(11) Song, J.-L.; Hu, C.-L.; Xu, X.; Kong, F.; Mao, J.-G. A Facile Synthetic Route to a New SHG Material with Two Types of Parallel π-Conjugated Planar Triangular Units. *Angew. Chem., Int. Ed.* **2015**, *54*, 3679−3682.

(12) Huang, H.; Tian, N.; Jin, S.; Zhang, Y.; Wang, S. Syntheses, characterization and nonlinear optical properties of a bismuth subcarbonate $Bi_2O_2CO_3$. *Solid State Sci.* **2014**, *30*, 1−5.

(13) Peltz, M.; Bartschke, J.; Borsutzky, A.; Wallenstein, R.; Vernay, S.; Salva, T.; Rytz, D. Harmonic generation in bismuth triborate (BiB_3O_6). *Appl. Phys. B: Lasers Opt.* **2005**, *81*, 487−495.

(14) (a) Frohlich, V. R.; Bohatý, L.; Liebertz, J. Die Kristallstruktur von Wismutborat, BiB_3O_6. *Acta Crystallogr., Sect. C: Cryst. Struct. Commun.* **1984**, *C40*, 343−344. (b) Cong, R.; Yang, T.; Liao, F.; Wang, Y.; Lin, Z.; Lin, J. Experimental and theoretical studies of

DOI: 10.1021/acs.inorgchem.7b00120
Inorg. Chem. 2017, 56, 5636−5645

second harmonic generation for $Bi_2O_2[NO_3(OH)]$. *Mater. Res. Bull.* **2012**, *47*, 2573−2578.
(15) Huang, Y.-Z.; Wu, L.-M.; Wu, X.-T.; Li, L.-H.; Chen, L.; Zhang, Y.-F. $Pb_2B_5O_9I$: An iodide Borate with Strong Second Harmonic Generation. *J. Am. Chem. Soc.* **2010**, *132*, 12788−12789.
(16) Cao, X.-L.; Hu, C.-L.; Xu, X.; Kong, F.; Mao, J.-G. $Pb_2TiOF(SeO_3)_2Cl$ and $Pb_2NbO_2(SeO_3)_2Cl$: small changes in structure induced a very large SHG enhancement. *Chem. Commun.* **2013**, *49*, 9965−9967.
(17) Liang, M.-L.; Hu, C.-L.; Kong, F.; Mao, J.-G. $BiFSeO_3$: An Excellent SHG Material Designed by Aliovalent Substitution. *J. Am. Chem. Soc.* **2016**, *138*, 9433−9436.
(18) Geng, L.; Li, Q.; Meng, C.-Y.; Dai, K.; Lu, H.-Y.; Lin, C.-S.; Cheng, W.-D. $BaBi(SeO_3)_2Cl$: a new polar material showing high second-harmonic generation efficiency enhanced by constructive alignment of chloride ions. *J. Mater. Chem. C* **2015**, *3*, 12290−12296.
(19) Sun, C.-F.; Hu, C.-L.; Mao, J.-G. PbPt $(IO_3)_6(H_2O)$: a new polar material with two types of stereoactive lone-pairs and a very large SHG response. *Chem. Commun.* **2012**, *48*, 4220−4222.
(20) Hu, W.; Shan, P.; Sun, T. Q.; Liu, H. D.; Zhang, J. M.; Liu, X. W.; Kong, Y. F.; Xu, J. J. Preparation, nonlinear optical properties, and theoretical analysis of the non-centrosymmetric bismuth oxyfluoride, $Bi_7F_{11}O_5$. *J. Alloys Compd.* **2016**, *658*, 788−794.
(21) Aliev, A.; Kovrugin, V. M.; Colmont, M.; Terryn, C.; Huvé, M.; Siidra, O. I.; Krivovichev, S. V.; Mentré, O. Revised Bismuth Chloroselenite System: Evidence of a Noncentrosymmmetric Structure with a Giant Unit Cell. *Cryst. Growth Des.* **2014**, *14*, 3026−3034.
(22) Geng, L.; Meng, C.; Lu, H.; Luo, Z.; Lin, C.; Cheng, W. $Bi_2Te(IO_3)O_5Cl$: a novel polar iodate oxychloride exhibiting a second-order nonlinear optical response. *Dalton Trans.* **2015**, *44*, 2469−2475.
(23) Zhang, G.; Wu, Y.; Li, Y.; Chang, F.; Pan, S. L.; Fu, P.; Chen, C. T. Flux growth and characterization of a new oxyborate crystal $Na_3La_9O_3(BO_3)_8$. *J. Cryst. Growth* **2005**, *275*, e1997−e2001.
(24) Wu, Y.; Liu, J.; Fu, P.; Wang, J.; Zhou, H.; Wang, G.; Chen, C. T. A new lanthanum and calcium borate $La_2CaB_{10}O_{19}$. *Chem. Mater.* **2001**, *13*, 753−755.
(25) Li, K.; Zhang, G.; Guo, S.; Zhang, X.; He, R.; Zhang, J.; Lin, Z.; Wu, Y. Linear and nonlinear optical properties of $Na_3La_2(BO_3)_3$ crystal. *Opt. Laser Technol.* **2013**, *54*, 407−412.
(26) Luo, M.; Ye, N.; Zou, G.; Lin, C.; Cheng, W. $Na_8Lu_2(CO_3)_6F_2$ and $Na_3Lu(CO_3)_2F_2$: Rare earth fluoride carbonates as deep-UV nonlinear optical materials. *Chem. Mater.* **2013**, *25*, 3147−3153.
(27) Liu, L.; Su, X.; Yang, Y.; Pan, S. L.; Dong, X.; Han, S.; Zhang, M.; Kang, J.; Yang, Z. H. $Ba_2B_{10}O_{17}$: a new centrosymmetric alkaline-earth metal borate with a deep-UV cut-off edge. *Dalton Trans.* **2014**, *43*, 8905−8910.
(28) Xu, K.; Loiseau, P.; Aka, G. $BaCaBO_3F$: A nonlinear optical crystal investigated for UV light generation. *J. Cryst. Growth* **2009**, *311*, 2508−2512.
(29) Hu, C.-L.; Xu, X.; Sun, C.-F.; Mao, J.-G. Electronic structures and optical properties of $Ca_5(BO_3)_3F$: asystematical first-principles study. *J. Phys.: Condens. Matter* **2011**, *23*, 395501.
(30) McMillen, C. D.; Stritzinger, J. T.; Kolis, J. W. Two Novel Acentric Borate Fluorides: $M_3B_6O_{11}F_2$ (M = Sr, Ba). *Inorg. Chem.* **2012**, *51*, 3953−3955.
(31) (a) Li, L.; Li, G.; Wang, Y.; Liao, F.; Lin, J. Bismuth Borates: One-dimensional Borate Chains and Nonlinear Optical Properties. *Chem. Mater.* **2005**, *17*, 4174−4180. (b) Cong, R.; Wang, Y.; Kang, L.; Zhou, Z.; Lin, Z.; Yang, T. An outstanding second-harmonic generation material BiB_2O_4F: exploiting the electron-withdrawing ability of fluorine. *Inorg. Chem. Front.* **2015**, *2*, 170−176.
(32) Rouse, J.; Redrup, K. V.; Kotsapa, E.; Weller, M. T. Controlling dimensionality in templated layer, chain and framework structures by combining metal fluorides with oxotetrahedra. *Chem. Commun.* **2009**, *46*, 7209−7211.
(33) Wu, H. P.; Yu, H. W.; Yang, Z. H.; Hou, X.; Su, X.; Pan, S. L.; Poeppelmeier, K. R.; Rondinelli, J. M. Designing a deep-ultraviolet nonlinear optical material with a large second harmonic generation response. *J. Am. Chem. Soc.* **2013**, *135*, 4215−4218.
(34) Zhang, H.; Zhang, M.; Pan, S. L.; Yang, Z. H.; Wang, Z.; Bian, Q.; Hou, X. L.; Yu, H. W.; Zhang, F. F.; Wu, K.; Yang, F.; Peng, Q. J.; Xu, Z. Y.; Chang, K. B.; Poeppelmeier, K. R. $Na_3Ba_2(B_3O_6)_2F$: Next Generation of Deep-Ultraviolet Birefringent Materials. *Cryst. Growth Des.* **2015**, *15*, 523−529.
(35) Reshak, A. H.; Huang, H.; Kamarudin, H.; Auluck, S. Alkali-metal/alkaline-earth-metal fluorine beryllium borate $NaSr_3Be_3B_3O_9F_4$ with large nonlinear optical properties in the deep-ultraviolet region. *J. Appl. Phys.* **2015**, *117*, 085703−085708.
(36) Yu, H. W.; Wu, H. P.; Pan, S. L.; Wang, Y.; Yang, Z. H.; Su, X. New Salt-Inclusion Borate, $Li_3Ca_9(BO_3)_7{\cdot}2[LiF]$: A Promising UV NLO Material with the Coplanar and High Density BO_3 Triangles. *Inorg. Chem.* **2013**, *52*, 5359−5365.
(37) Kokh, A.; Simonova, E.; Maillard, A.; Maillard, R.; Svetlichnyi, V.; Andreev, Y.; Kragzhda, A.; Kuznetsov, A.; Kokh, K. Growth and dichroic properties of $LiBa_{12}(BO_3)_7F_4$ crystal. *Cryst. Res. Technol.* **2016**, *51*, 530−533.
(38) Belokoneva, E. L.; Stefanovich, S. Y.; Erilov, M. A.; Dimitrova, O. V.; Mochenova, N. N. A New Modification of $Ba[B_5O_8(OH)]{\cdot}H_2O$, the Refined Structure of $Ba_2[B_5O_9]Cl{\cdot}0.5H_2O$, and the Role of the Pentaborate Structural Units in the Formation of the Quadratic Optical Nonlinearity. *Crystallogr. Rep.* **2008**, *53*, 228−236.
(39) Chen, C. T.; Ye, N.; Lin, J.; Jiang, J.; Zeng, W.; Wu, B. Computer-Assisted Search for Nonlinear Optical Crystals. *Adv. Mater.* **1999**, *11*, 1071−1078.
(40) Lo, C.-h. Master's Degree Thesis, The Role of Electron Lone-pair in the Optical Nonlinearity of Oxide, Nitride and Halide Crystals, Tamkang University, 2005.
(41) Lee, M.-H.; Yang, C.-H.; Jan, J.-H. Band-resolved analysis of nonlinear optical properties of crystalline and molecular materials. *Phys. Rev. B: Condens. Matter Mater. Phys.* **2004**, *70*, 235110−235121.
(42) (a) Clark, S. J.; Segall, M. D.; Pickard, C. J.; Hasnip, P. J.; Probert, M. I. J.; Refson, K.; Payne, M. C. First principles methods using CASTEP. *Z. Kristallogr. - Cryst. Mater.* **2005**, *220*, 567−570. (b) Milman, V.; Refson, K.; Clark, S. J.; Pickard, C. J.; Yates, J. R.; Gao, S.-P.; Hasnip, P. J.; Probert, M. I. J.; Perlov, A.; Segall, M. D. Electron and vibrational spectroscopies using DFT, plane waves and pseudopotentials: CASTEP implementation. *J. Mol. Struct.: THEOCHEM* **2010**, *954*, 22−35.
(43) (a) Hohenberg, P.; Kohn, W. Inhomogeneous electron gas. *Phys. Rev.* **1964**, *136*, B864−B871. (b) Ceperley, D. M.; Alder, B. J. Ground State of the Electron gas by a Stochastic method. *Phys. Rev. Lett.* **1980**, *45*, 566−569.
(44) (a) Burke, K.; Ernzerhof, M.; Perdew, J. P. The adiabatic connection method: a non-empirical hybrid. *Chem. Phys. Lett.* **1997**, *265*, 115−120. (b) Perdew, J. P.; Burke, K.; Ernzerhof, M. Generalized Gradient Approximation Made Simple. *Phys. Rev. Lett.* **1996**, *77*, 3865−3868. (c) Vanderbilt, D. Soft self-consistent pseudopotentials in a generalized eigenvalue formalism. *Phys. Rev. B: Condens. Matter Mater. Phys.* **1990**, *41*, 7892−7895.
(45) Monkhorst, H. J.; Pack, J. D. Special points for Brillouin-zone integrations. *Phys. Rev. B* **1976**, *13*, 5188−5192.
(46) (a) Levine, Z. H.; Allan, D. C. Quasiparticle calculation of the dielectric response of silicon and germanium. *Phys. Rev. B: Condens. Matter Mater. Phys.* **1991**, *43*, 4187−4207. (b) Cohen, A. J.; Mori-Sánchez, P.; Yang, W. Insights into current limitations of density functional theory. *Science* **2008**, *321*, 792−794.
(47) Levine, Z. H.; Allan, D. C. Linear Optical Response in Silicon and Germanium Including Self-Energy Effects. *Phys. Rev. Lett.* **1989**, *63*, 1719−1722.
(48) Zhang, B. B.; Lee, M.-H.; Yang, Z. H.; Jing, Q.; Pan, S. L.; Zhang, M.; Wu, H. P.; Su, X.; Li, C.-S. Simulated pressure-induced blue-shift of phase-matching region and nonlinear optical mechanism for $K_3B_6O_{10}X$ (X= Cl, Br). *Appl. Phys. Lett.* **2015**, *106*, 031906.
(49) (a) Lei, B.-H.; Jing, Q.; Yang, Z. H.; Zhang, B. B.; Pan, S. L. Anomalous Second Harmonic Generation (SHG) response in $SrBPO_5$ and $BaBPO_5$. *J. Mater. Chem. C* **2015**, *3*, 1557−1566. (b) Li, L.-P.;

DOI: 10.1021/acs.inorgchem.7b00120
Inorg. Chem. 2017, 56, 5636−5645

Yang, Z. H.; Lei, B.-H.; Kong, Q.; Lee, M.-H.; Zhang, B. B.; Pan, S. L.; Zhang, J. Active performance of tetrahedral groups to SHG response: theoretical interpretations of Ge/Si-containing borate crystals. *Phys. Chem. Chem. Phys.* **2016**, *18*, 6077−6084. (c) Bashir, B.; Zhang, B. B.; Lei, B.-H.; Yang, Z. H.; Lee, M.-H.; Pan, S. L. DFT Based Theoretical Study about the Contributions of Fluorine to Nonlinear Optical Properties in Borate Fluoride Crystals. *Cryst. Growth Des.* **2016**, *16*, 5067−5073.

(50) (a) Wang, S.; Alekseev, E. V.; Diwu, J.; Miller, H. M.; Oliver, A. G.; Liu, G.; Depmeier, W.; Albrecht-Schmitt, T. E. Functionalization of Borate Networks by the Incorporation of Fluoride: Syntheses, Crystal Structures, and Nonlinear Optical Properties of Novel Actinide Fluoroborates. *Chem. Mater.* **2011**, *23*, 2931−2939. (b) Cakmak, G.; Nuss, J.; Jansen, M. LiB_6O_9F, the First Lithium Fluorooxoborate−Crystal Structure and Ionic Conductivity. *Z. Anorg. Allg. Chem.* **2009**, *635*, 631−636. (c) Zhang, B. B.; Shi, G.; Yang, Z. H.; Zhang, F. F.; Pan, S. L. Fluorooxoborates: Beryllium-Free Deep-Ultraviolet Nonlinear Optical Materials without Layered Growth. *Angew. Chem., Int. Ed.* **2017**, *56*, 3916−3919.

(51) Barbier, J.; Cranswick, L. M. D. The non-centrosymmetric borate oxides, $MBi_2B_2O_7$ (M= Ca, Sr). *J. Solid State Chem.* **2006**, *179*, 3958−3964.

(52) Barbier, J.; Penin, N.; Denoyer, A.; Cranswick, L. M. D. $BaBiBO_4$, a novel non-centrosymmetric borate oxide. *Solid State Sci.* **2005**, *7*, 1055−1061.

(53) Jing, Q.; Yang, Z. H.; Pan, S. L.; Xue, D.-F. Contribution of lone-pairs to birefringence affected by the Pb(II) coordination environment: a DFT investigation. *Phys. Chem. Chem. Phys.* **2015**, *17*, 21968−21973.

(54) Zhao, W.-W.; Pan, S. L.; Han, J.; Yao, J.; Yang, Y.; Li, J.; Zhang, M.; Zhang, L. H.; Hang, Y. Synthesis, crystal structure and optical properties of the new lead fluoride borate—Pb_2BO_3F. *J. Solid State Chem.* **2011**, *184*, 2849−2853.

(55) Lu, H.; Gautier, R.; Donakowski, M. D.; Tran, T. T.; Edwards, B. W.; Nino, J. C.; Halasyamani, P. S.; Liu, Z.; Poeppelmeier, K. R. Nonlinear Active Materials: An Illustration of Controllable Phase Matchability. *J. Am. Chem. Soc.* **2013**, *135*, 11942−11950.

(56) Shi, R.; Huang, G.; Lin, J.; Zhu, Y. Photocatalytic activity enhancement for Bi_2WO_6 by fluorine substitution. *J. Phys. Chem. C* **2009**, *113*, 19633−19638.

(57) Zhang, M.; Su, X.; Mutailipu, M.; Yang, Z. H.; Pan, S. L. $Bi_3OF_3(IO_3)_4$: The First Metal Oxyiodate Fluoride Featuring a Carbon-nanotube-like Topological Structure with Large SHG Response. *Chem. Mater.* **2017**, *29*, 945−949.

(58) Donakowski, M. D.; Gautier, R.; Lu, H.; Tran, T. T.; Cantwell, J. R.; Halasyamani, P. S.; Poeppelmeier, K. R. Syntheses of Two Vanadium Oxide−Fluoride Materials That Differ in Phase Matchability. *Inorg. Chem.* **2015**, *54*, 765−772.

(59) Tong, Y.; Meng, X. Y.; Wang, Z. Z.; Chen, C. T.; Lee, M.-H. The mechanism of linear and nonlinear optical effects in fluoride crystals. *J. Appl. Phys.* **2005**, *98*, 033504−7.

(60) (a) Pandith, A. H.; Islam, N. Electron Transport and Nonlinear Optical Properties of Substituted Aryldimesityl Boranes: A DFT Study. *PLoS ONE* **2014**, *9*, e114125. (b) Janjua, M. R. S. A. Quantum Mechanical Design of Efficient Second-Order Nonlinear Optical Materials Based on Heteroaromatic Imido-Substituted Hexamolybdates: First Theoretical Framework of POM-Based Heterocyclic Aromatic Rings. *Inorg. Chem.* **2012**, *51*, 11306−11314.

(61) Rocquefelte, X.; Goubin, F.; Montardi, Y.; Viadere, N.; Demourgues, A.; Tressaud, A.; Whangbo, M.-H.; Jobic, S. Analysis of the Refractive Indices of TiO_2, $TiOF_2$, and TiF_4: Concept of Optical Channel as a Guide To Understand and Design Optical Materials. *Inorg. Chem.* **2005**, *44*, 3589−3593.

(62) Egorova, B. V.; Olenev, A. V.; Berdonosov, P. S.; Kuznetsov, A. N.; Stefanovich, S. Y.; Dolgikh, V. A.; Mahenthirarajah, T.; Lightfoot, P. Lead−strontium borate halides with hilgardite-type structure and their SHG properties. *J. Solid State Chem.* **2008**, *181*, 1891−1898.

(63) Hoffmann, R. How chemistry and physics meet in the solid state. *Angew. Chem., Int. Ed. Engl.* **1987**, *26*, 846−878.

(64) (a) Payne, D. J.; Egdell, R. G.; Walsh, A.; Watson, G. W.; Guo, J.; Glans, P.-A.; Learmonth, T.; Smith, K. E. Electronic Origins of Structural Distortions in Post-Transition Metal Oxides: Experimental and Theoretical Evidence for a Revision of the Lone Pair Model. *Phys. Rev. Lett.* **2006**, *96*, 157403. (b) Walsh, A.; Payne, D. J.; Egdell, R. G.; Watson, G. W. Stereochemistry of post-transition metal oxides: revision of the classical lone pair model. *Chem. Soc. Rev.* **2011**, *40*, 4455−4463.

(65) Li, D.; Jing, Q.; Lei, C.; Pan, S. L.; Zhang, B. B.; Yang, Z. H. Theoretical perspective of the lone pair activity influence on band gap and SHG response of lead borates. *RSC Adv.* **2015**, *5*, 79882−79887.

■ NOTE ADDED AFTER ASAP PUBLICATION

This paper was published on the Web on April 27, 2017, with errors in the TOC and Abstract graphic. The corrected version was reposted on April 28, 2017.

DOI: 10.1021/acs.inorgchem.7b00120
Inorg. Chem. 2017, 56, 5636−5645